Transverse diaphragms and unbonded CFRP post-tensioning in box-beam bridges

Nabil F. Grace,
Elin A. Jensen,
Tsuyoshi Enomoto,
Vasant A. Matsagar,
Eslam M. Soliman,
and Joseph Q. Hanson

Editor's quick points

- Carbon-fiber-reinforced-polymer (CFRP) strands alleviate many construction challenges when used as transverse post-tensioning in box-beam bridges.
- The use of unbonded transverse post-tensioning of CFRP strands for replacement of strands that are damaged or deteriorated is considered.
- The results of testing of a model using transverse, post-tensioned CFRP strands are presented.

Longitudinal cracking in deck slabs over shear keys is a common distress in prestressed concrete box-beam highway bridges. These cracks can be initiated by a drastic thermal gradient and are further propagated as a result of traffic loads. Longitudinal cracks can also develop because of differential rotation between the adjacent box beams due to eccentric application of the service load.[1] In addition, long-term neglect of preventive maintenance, improper handling during production and construction, and inadequate shear-key performance can cause longitudinal cracks in concrete deck slabs.[2] Furthermore, the longitudinal cracks, combined with the excessive relative vertical displacements between the adjacent box beams, lead to failure of the shear key.[3]

The longitudinal cracks may compromise the waterproofing action of the deck and allow water and chemicals to penetrate through the concrete, causing steel corrosion and eventually reducing the serviceability and longevity of the bridge.[4] Corroded steel may cause additional cracking and can lead to spalling of the concrete in the surrounding area.

The use of transverse post-tensioning force has been considered a viable method of preventing the development of longitudinal cracks in the deck slab of box-beam bridges. Furthermore, the misalignment of the transverse post-tensioning ducts due to differential cambers in adjacently placed box beams poses a great construction challenge. Alternatively, carbon-fiber-reinforced-polymer

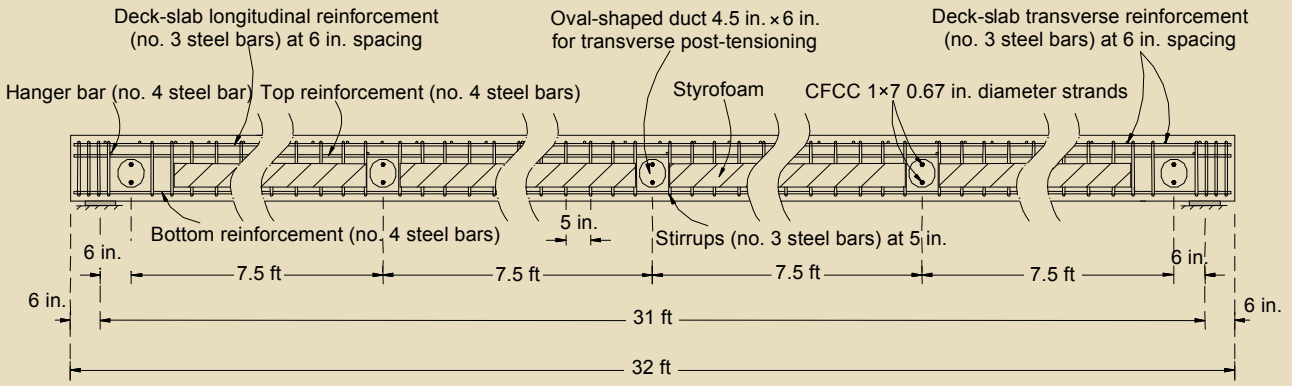

Figure 1. This diagram shows the longitudinal section of the bridge model. Note: 1 in. = 25.4 mm; 1 ft = 0.305 m; no. 3 = 10M; no. 4 = 13M.

(CFRP) strands have advantages over the conventional steel strands, such as greater longitudinal axial strength, less thermal expansion, and less density.[5] Because they are noncorrosive, CFRP strands are considered suitable for prestressed concrete bridges in moderate to aggressive environments.[6] The use of unbonded CFRP strands for transverse post-tensioning has been successfully implemented in the field with the construction of the Bridge Street Bridge, the first three-span CFRP prestressed concrete highway bridge in the United States.[7]

Another major issue in current construction practice for side-by-side box-beam bridges is the replacement of damaged or deteriorated exterior or interior beams. In prestressed concrete highway bridges, a high-impact load on the fascia box beams is potentially induced by collision of overheight vehicles.[8] Damage resulting from a collision by an overheight vehicle may require replacement of the entire superstructure when individual beams cannot practically be replaced. In side-by-side precast, prestressed concrete box-beam bridges, replacing a damaged beam is challenging when bonded transverse post-tensioning steel strands are used. The use of unbonded transverse post-tensioning strands could be an alternative to using the bonded strands in side-by-side box-beam bridges.

To address these problems, the Michigan Department of Transportation (MDOT) funded an extensive experimental investigation as conducted on a half-scale, 30-deg-skew, precast, prestressed concrete side-by-side box-beam bridge model. The bridge model was constructed, instrumented, and tested using unbonded, transverse post-tensioned CFRP strands. Strain- and load-distribution tests were conducted to evaluate the effect of the level of transverse post-tensioning forces and the number of diaphragms on the behavior of the bridge model in the transverse direction.

This paper presents the details of the construction, experimental test procedures, discussions of the test results, and conclusions on the bridge model. Noncorrosive unbonded carbon-fiber-composite-cable (CFCC) strands were examined and recommended for their use as transverse post-tensioning strands. The results of this research investigation quantify the influence of the level of transverse post-tensioning force and the number of transverse diaphragms on improving the deformation response of side-by-side box-beam bridges.

In addition, a practical and simple approach for the replacement of a damaged beam was proposed and successfully implemented. Currently, MDOT is scheduling the deployment of the results of this investigation in a two-span, box-beam bridge that will be constructed in 2010 over highway M-39 in Michigan.

Experimental investigation

A half-scale, 30-deg-skewed, precast, prestressed concrete side-by-side box-beam bridge model was designed and constructed in the Center for Innovative Materials Research at Lawrence Technological University. The bridge model consisted of four precast, prestressed concrete box beams designated as B-1, B-2, B-3, and B-4. The box beams were placed side by side to form full-depth female-to-female keyways that facilitated the construction of the shear keys.

In addition, five transverse diaphragms were provided at an equal spacing of 7.5 ft (2.3 m) according to MDOT specifications.[9] A 3-in.-thick (75 mm) reinforced deck slab was placed over the box beams. The span of the bridge model was 31 ft (9.5 m). **Figures 1** and **2** show the longitudinal and cross-section details of the bridge model.

Bridge-model construction

The top and bottom reinforcement for each box beam consisted of four no. 4 (13 M) deformed steel reinforcing bars. In addition, three 0.5-in.-diameter (13 mm), seven-

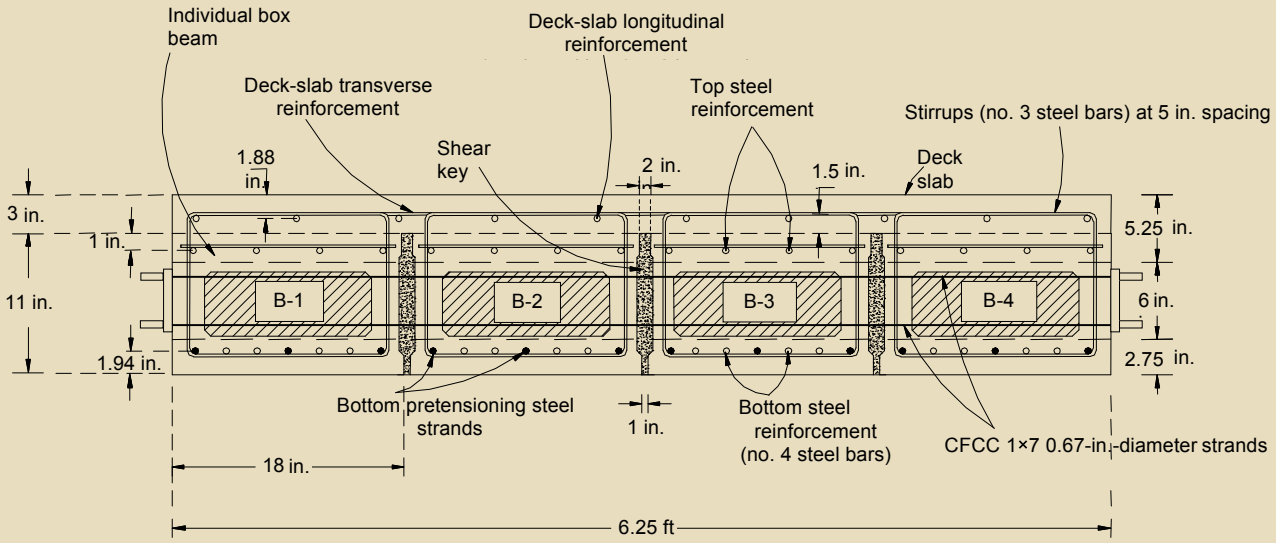

Figure 2. This drawing illustrates the cross section of the bridge model. Note: 1 in. = 25.4 mm; 1 ft = 0.305 m; no. 3 = 10M; no. 4 = 13M.

wire steel prestressing strands were provided. The stirrups protruded 1.5 in. (38 mm) from the top surface of the box beams to achieve composite action between the box beams and deck slab.

To account for potential differential camber between the adjacent box beams, an oval-shaped duct was introduced at each transverse diaphragm to accommodate the unbonded transverse post-tensioning CFCC strands rather than the traditional circular duct. The oval-shaped ducts were created by inserting aluminum tubes at the appropriate transverse diaphragm locations. Pieces of 5-in.-deep (127 mm), 10-in.-wide (250 mm) Styrofoam were used to create the hollow portion within the cross section of the box beams and were placed at the midheight of the box-beam cross section.

To simulate differential camber commonly observed in the field, different levels of prestressing forces were applied to the individual box beams. The two exterior box beams were prestressed with an average force of 20 kip/strand (90 kN/strand), while the two interior box beams were prestressed with an average force of 25 kip/strand (111 kN/strand).

The box beams were cast from concrete with average 28-day compressive strength of 6300 psi (43 MPa). Styrofoam gaskets were attached at the ends of each transverse duct between the adjacent box beams to avoid the possible leakage of shear-key grout into the ducts.

The 3-in.-thick (75 mm) cast-in-place concrete deck slab was reinforced with no. 3 (10M) deformed steel reinforc-

Table 1. Characteristics of CFCC strands and steel reinforcement

	Grade	Nominal diameter, in.	Effective cross-sectional area, in.^{2}	Linear density, lb/in.	Minimum yield strength, ksi	Breaking load, kip	Tensile strength, ksi	Tensile modulus, ksi	Elongation at break
CFCC seven-wire strands*	n.a.	0.67	0.23	16.2	n.a.	78.4	0.34	22.3	1.5
Nonprestressing steel no. 4 bar	60	0.5	0.2	8.0	60	18.0	90	29,000	9
Seven-wire steel prestressing strands	270	0.5	0.153	6.24	229.5	41.3	250	27,000	1
Steel stirrups, no. 3 bars	60	0.375	0.11	4.512	60	9.9	90	29,000	9

* Data are from Tokyo Rope Mfg. Co. Ltd., *CFCC Quality Report* (2007).

Note: CFCC = carbon-fiber-composite cable; n.a. = not applicable. 1 in. = 25.4 mm; 1 lb = 4.448 N; 1 kip = 4.448 kN; 1 ksi = 6.895 MPa; no. 3 = 10M; no. 4 = 13M.

Figure 3. This photo depicts the general view of the precast, prestressed concrete box-beam bridge model.

ing bars spaced at 6 in. (150 mm) center-to-center in the longitudinal and transverse directions. The deck slab was cast using concrete with a 28-day average compressive strength of 4600 psi (32 MPa). The CFRP reinforcement used for transverse post-tensioning was 0.67-in.-diameter (17 mm) CFCC seven-wire strands. **Table 1** shows the mechanical properties of the CFCC strands and steel reinforcement. **Figure 3** shows the completed bridge model.

Test program

The test program was conducted in three distinct phases similar to what a highway box-beam bridge might experience during its service life span.

Uncracked deck slab (UC) The uncracked concrete deck-slab phase was used as a reference phase for the investigation. This phase simulated a typical newly constructed highway bridge without any longitudinal cracks. Both load- and strain-distribution tests were conducted at this phase.

Cracked deck slab (C) In this phase, the concrete deck slab and the shear keys were partially cracked, simulating the longitudinal cracks developed in the deck over the shear keys. The longitudinal cracks were initiated by applying a single point load to individual beams while partially restraining the other three beams.

Damaged-beam replacement (R) This phase involved the replacement of an assumed damaged exterior box beam with a new box beam, new shear key, and portion of a reinforced deck slab tied to the existing concrete deck slab. The replacement procedure involved several steps:

1. A full-depth cut was made in the exterior shear key C-C (**Fig. 4**) between box beams B-3 and B-4.
2. Horizontal 0.75-in.-diameter (19 mm), 12-in.-deep (300 mm) holes were drilled into the deck slab using an electric hammer drill to accommodate the new concrete deck slab's transverse reinforcement.
3. The new exterior beam B-5 was placed adjacent to box beam B-3, and the shear key between the two beams was grouted.
4. The concrete deck slab's longitudinal reinforcement was placed and tied at an equal spacing of 6 in. (150 mm) center to center, and its transverse reinforcement was placed in the holes with a high-performance epoxy resin.[10]
5. The deck-slab formwork was then constructed, followed by casting of the deck slab with the same mixture proportions used for casting the original concrete deck slab.

Three major tests were conducted on the bridge model: transverse strain distribution, load distribution, and ulti-

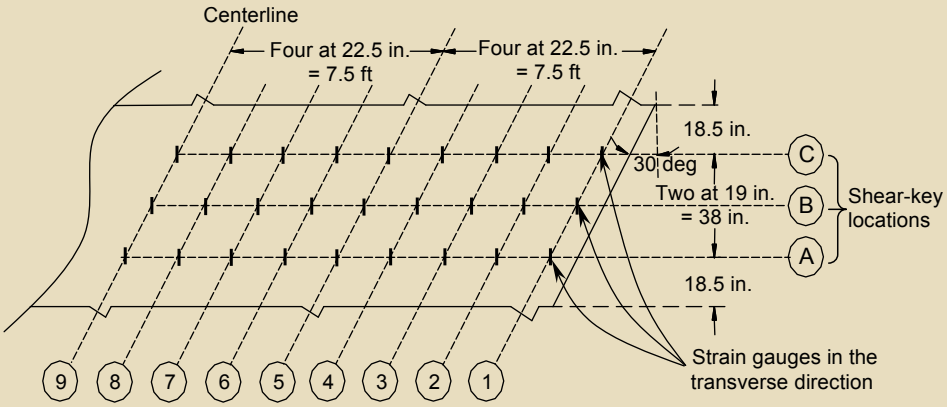

Figure 4. This diagram shows the shear-key locations and strain-gauge layout on the deck slab. Note: 1 in. = 25.4 mm; 1 ft = 0.305 m.

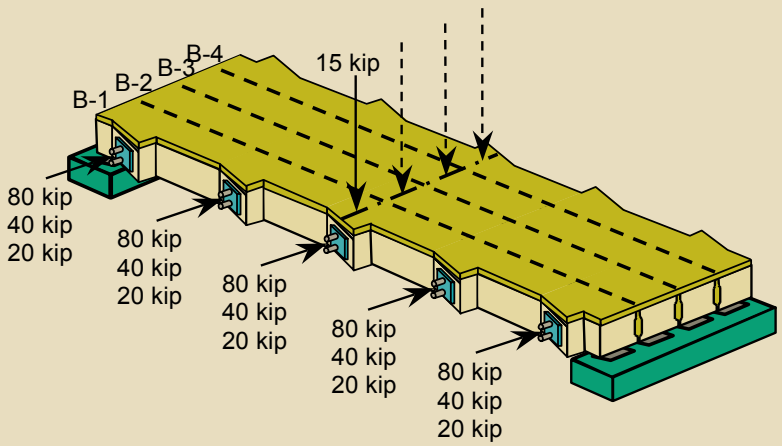

Figure 5. The load-distribution test applies transverse post-tensioning forces at five diaphragms. Note: 1 kip = 4.448 kN.

mate load. Following are the procedures used during the tests.

Transverse-strain-distribution test The strain-distribution test was conducted by applying different levels of transverse post-tensioning forces at different diaphragms using unbonded CFCC strands. This test was conducted during the uncracked-deck-slab phase only. The transverse strains were monitored using 27 strain gauges installed on the top surface of the deck slab at the shear-key locations and oriented in the transverse direction (Fig. 4). Two unbonded CFCC strands provided transverse post-tensioning forces at each diaphragm.

Four levels of transverse post-tensioning forces were selected: 0 kip, 20 kip, 40 kip, and 80 kip (0 kN, 90 kN, 180 kN, and 360 kN). These forces were applied at each diaphragm and were distributed equally between the two CFCC strands. These transverse post-tensioning force levels were varied along with number of diaphragms receiving the forces (three to five diaphragms). In the three-diaphragm case, the transverse post-tensioning forces were applied at the midspan and end diaphragms. In the four-diaphragm case, the transverse post-tensioning forces were applied at the quarter-span and end diaphragms. In the five-diaphragm case, the transverse post-tensioning forces were applied at all five diaphragms.

Load-distribution test The load-distribution test was conducted by applying a single point load of 15 kip (67 kN) on each box beam at the midspan for different arrangements of the transverse post-tensioning forces. This load level was selected to avoid potential cracking problems. The corresponding deflections were recorded using linear-motion transducers attached at the midspan of all box beams. **Figure 5** shows the arrangement of the load-distribution test for the case of five diaphragms. The load-distribution test was conducted on all three phases of the test program.

Ultimate-load test The ultimate-load test was conducted to determine the ultimate flexural load-carrying capacity of the bridge model and to evaluate the response of the unbonded transverse post-tensioning CFCC strands up to failure of the bridge model. A transverse post-tensioning force of 80 kip (360 kN) was applied at all five diaphragms before testing. The bridge model was loaded eccentrically at the midspan of box beam B-2 using a two-point loading frame (**Fig. 6**).

The transverse post-tensioning forces were monitored during the test using load cells attached to the dead end of the CFCC strands. Four linear-motion transducers were also installed at the midspan of each box beam to monitor the corresponding deflections. Five loading and unloading cycles were conducted before failure by increasing and releasing the applied load at a rate of about 15 kip/min (67 kN/min).

Experimental results and discussion

The results of the load- and strain-distribution tests were used to evaluate the effect of the level of transverse post-tensioning forces and number of diaphragms that the force was applied to on the behavior of the bridge model in the transverse direction. In addition, the results of the ultimate-load test were used to evaluate the response of the unbonded transverse post-tensioning arrangement during catastrophic failure.

Strain-distribution test

Effect of transverse post-tensioning force level on strains It was observed that by increasing the levels of the transverse post-tensioning forces, the transverse strains increased proportionally at all points located along the transverse diaphragms (**Fig. 7**). For example,

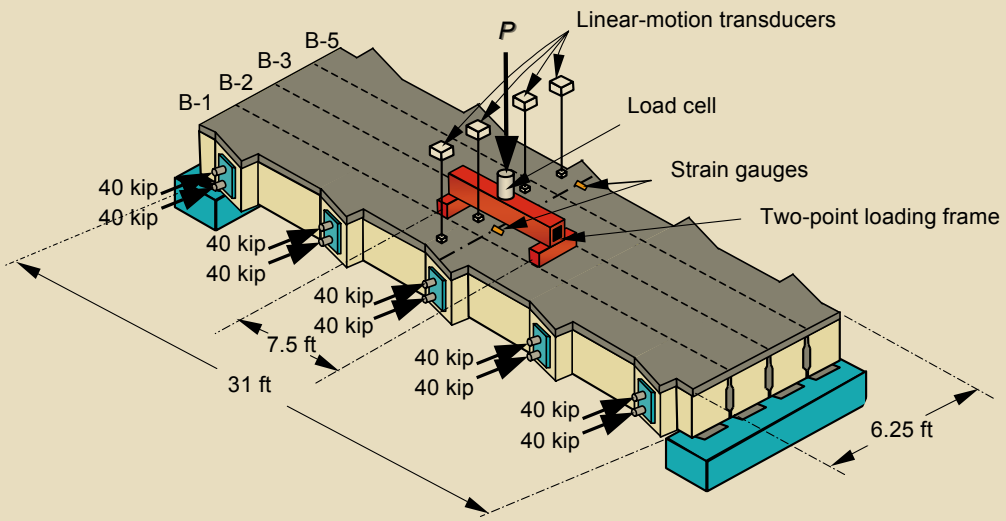

Figure 6. The experimental-setup ultimate-load test of the bridge model included a two-point loading frame, linear-motion transducers, and strain gauges. Note: AASHTO LRFD = The American Association of State and Highway Transportation Officials' *AASHTO LRFD Bridge Design Specifications*. 1 ft = 0.305 m; 1 kip = 4.448 kN.

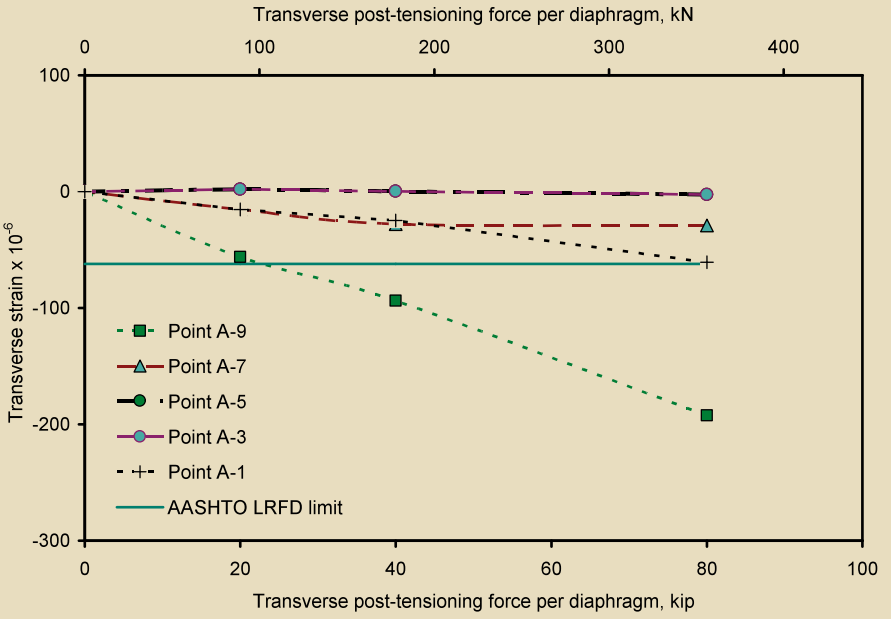

Figure 7. This graph shows the transverse strains along shear key A-A for transverse post-tensioning forces at five diaphragms.

for the case of five diaphragms, point A-9 (Fig. 4), located on the midspan diaphragm, experienced transverse strains of -192×10^{-6}, -94×10^{-6}, and -56×10^{-6} due to transverse post-tensioning forces of 80 kip, 40 kip, and 20 kip (360 kN, 180 kN, and 90 kN), respectively. Similar behavior was observed in the cases of three and four diaphragms.[11] The linear relation between the transverse post-tensioning forces and the corresponding transverse strains indicated an elastic behavior of the deck-slab concrete.

Effect of number of diaphragms on strains

As expected, for the case of five diaphragms the points located over the transverse diaphragms experienced higher transverse strains relative to those located between the diaphragms (**Fig. 8**), where the spacing between the transverse post-tensioning forces was 7.5 ft (2.3 m). For instance, point A-5, located over the quarter-span diaphragm, experienced a transverse strain of -87×10^{-6} due to a transverse post-tensioning force of 80 kip (360 kN) applied at each of the four diaphragms. Alternatively, point A-3, located between the quarter-span and end diaphragms, experienced

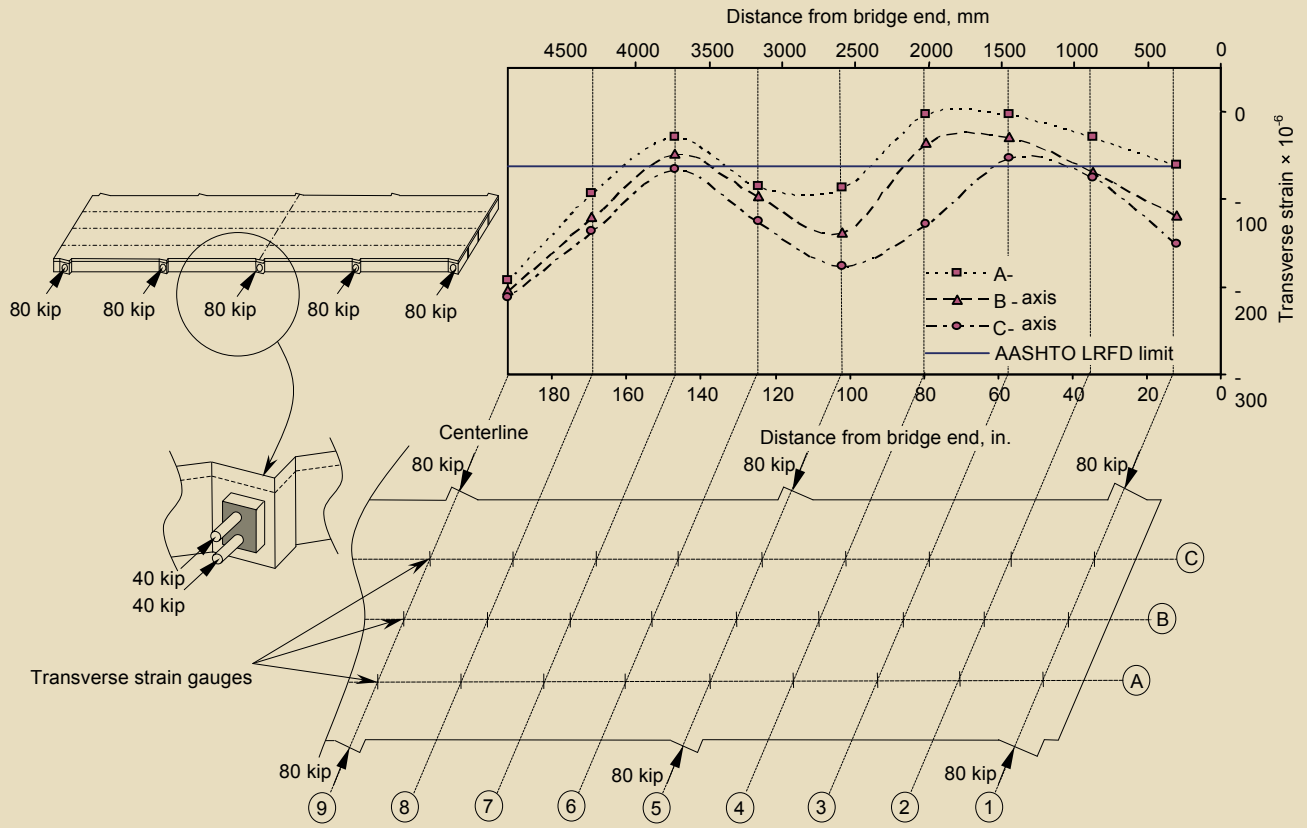

Figure 8. This graph shows the transverse strain distribution for a transverse post-tensioning force of 80 kip applied at five diaphragms. Note: AASHTO LRFD = The American Association of State and Highway Transportation Officials' *AASHTO LRFD Bridge Design Specifications*. 1 kip = 4.448 kN.

insignificant transverse strain due to the same arrangement of transverse post-tensioning forces.

Similar behavior was observed when 20 kip and 40 kip (90 kN and 180 kN) transverse post-tensioning forces were applied.[12] This was attributed to the nonuniform distribution of the transverse post-tensioning forces along the span of the bridge model, resulting in high local transverse strains in the regions near the diaphragms. In the case of four diaphragms (**Fig. 9**), where the transverse post-tensioning forces were applied to the quarter-span diaphragms at a spacing of 15 ft (4.6 m), low transverse strains were observed at the midspan region, and high transverse strains were observed at the end and quarter-span diaphragms. In general, the bridge model experienced the highest transverse strains near the transverse post-tensioning force locations, and the transverse strains decreased as the distance from the transverse post-tensioning forces increased.

Comparison with AASHTO LRFD recommendations The American Association of State Highway and Transportation Officials' (AASHTO's) *AASHTO LRFD Bridge Design Specifications* recommend a minimum transverse prestress of 0.25 ksi (1.7 MPa) developed due to transverse post-tensioning forces,[13] herein called the AASHTO LRFD specifications limit. However, the AASHTO LRFD specifications did not provide further details about the region or the area at which the limit should be maintained. To compare the measured transverse strains with the AASHTO LRFD specifications limit, it was converted to an equivalent limit of 62×10^{-6} and compared with the measured strains at the deck slab (Fig. 7).

It was observed that at least eight points experienced transverse strains below 62×10^{-6} for each arrangement of the transverse post-tensioning forces (Fig. 8). Furthermore, all of the 27 points experienced transverse strains less than that of the AASHTO LRFD specifications limit when the transverse post-tensioning force of 20 kip (90 kN) was applied. This was mainly because of the nonuniform distribution of the transverse post-tensioning forces along the span or inadequate levels of transverse post-tensioning forces. Similar trends were observed for the transverse strains when the same transverse post-tensioning force levels were applied through three and four diaphragms.

Load-distribution test

Effect of level of transverse post-tensioning forces The loaded beam always experienced the largest deflection, and the deflection in the other beams decreased as distance from the loaded beam increased. This was true

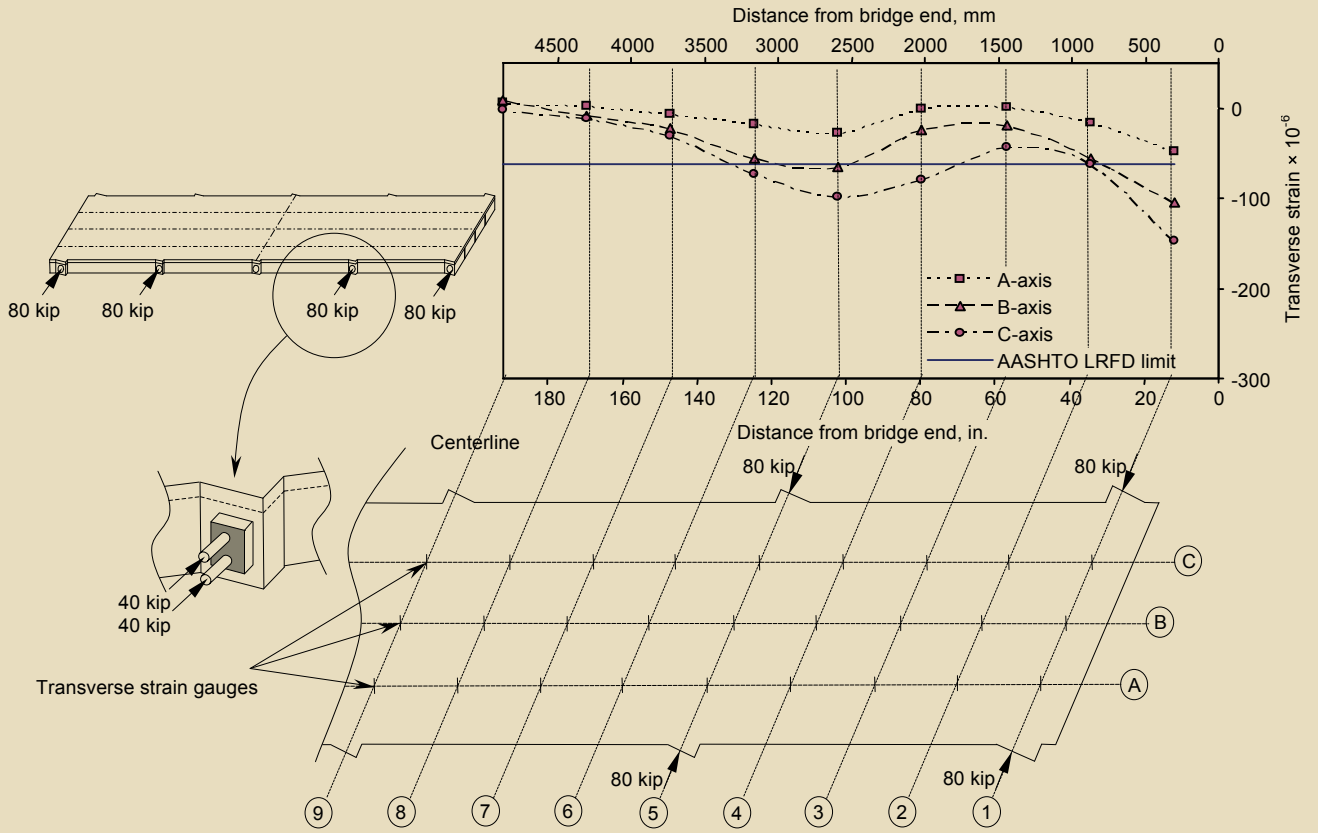

Figure 9. This graph shows the transverse strain distribution for a transverse post-tensioning force of 80 kip applied at four diaphragms. Note: AASHTO LRFD = The American Association of State and Highway Transportation Officials' *AASHTO LRFD Bridge Design Specifications*. 1 kip = 4.448 kN.

in both the cracked and repaired phases (**Fig. 10** and **11**). It was observed that the differences in these deflections decreased as the level of transverse post-tensioning forces increased. For instance, when box beam B-4 was loaded in the cracked phase and different levels of the transverse post-tensioning forces were applied at all five diaphragms, the differences in deflection between box beams B-1 and B-4 were 0.22 in., 0.05 in., 0.04 in., and 0.03 in. (5.59 mm, 1.27 mm, 1.02 mm, and 0.76 mm) for the transverse post-tensioning forces of 0 kip, 20 kip, 40 kip, and 80 kip (0 kN, 90 kN, 180 kN, and 360 kN), respectively.

Similarly, the differences in deflections in the repaired phase were 0.17 in., 0.05 in., 0.05 in., and 0.03 in. (4.32 mm, 1.27 mm, 1.27 mm, and 0.76 mm) for the same levels of the transverse post-tensioning forces. Moreover, the deflection of box beams B-3 and B-5 was reduced in the beam-replacement phase compared with the cracked-deck-slab phase (Fig. 10). This is attributed to increased stiffness caused by beam replacement and repair of the shear key and deck slab.

Furthermore, the deflections of the loaded interior beams were lower than that of the loaded exterior beam regardless of the level of transverse post-tensioning force and the phase of the bridge model (Fig. 10 and 11). The deflections observed in the cracked phase, when transverse post-tensioning forces of 0 kip, 20 kip, 40 kip, and 80 kip (0 kN, 90 kN, 180 kN, 360 kN) were applied to five diaphragms, were 0.42 in., 0.34 in., 0.33 in., and 0.30 in. (10.67 mm, 8.64 mm, 8.38 mm, and 7.62 mm) for the loaded exterior beam B-4 and 0.36 in., 0.32 in., 0.31 in., and 0.29 in. (9.14 mm, 8.13 mm, 7.87 mm, and 7.37 mm) for the loaded interior beam B-2. This clearly shows that increasing the transverse post-tensioning forces significantly improved the load distribution among the adjacent beams in the cracked and repaired phases.

In addition, it could be deduced that applying a transverse post-tensioning force of 40 kip (180 kN) is adequate to hold the adjacent beams to act as a unit when the bridge model was subjected to the vertical load. However, it did not satisfy the AASHTO LRFD specifications limit of 0.25 ksi (1.7 MPa).

Effect of number of diaphragms

Figures 12 and **13** show the effect of the number of transverse diaphragms on the deflection of the bridge model. The number of diaphragms did not affect the differences in deflection between the loaded beam and the far exterior box beam in the uncracked-deck-slab phase. However, for the cracked and beam-replacement phases, the three- and five-diaphragm

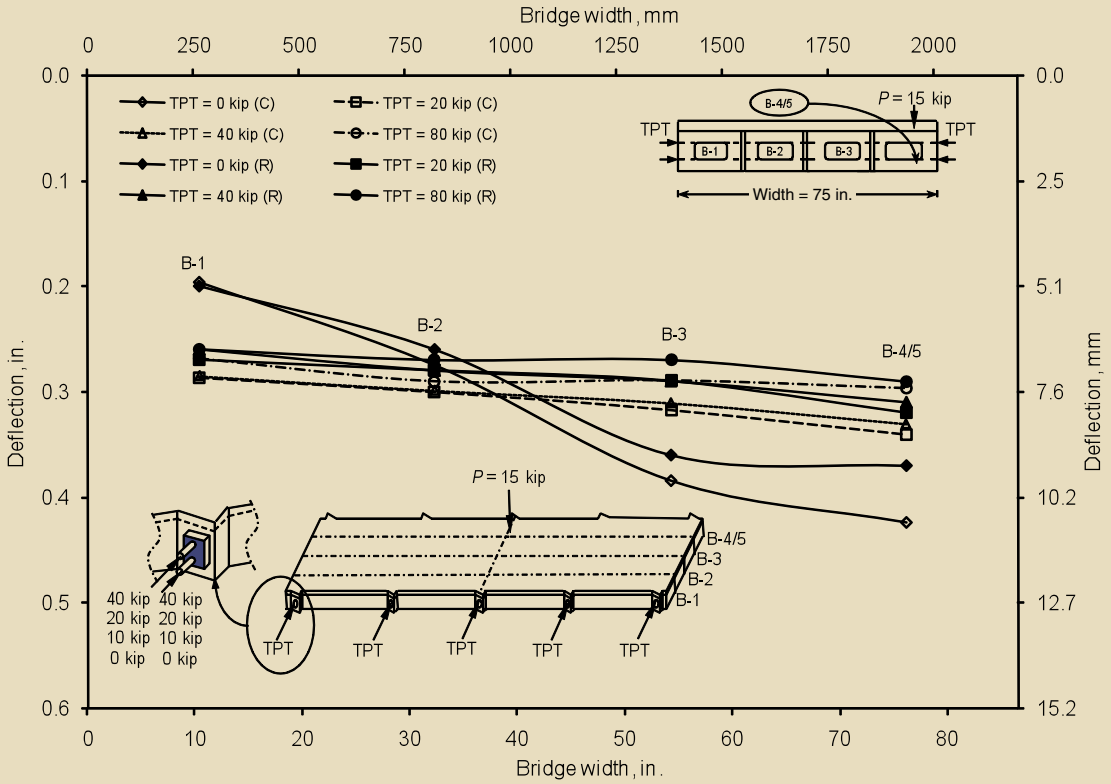

Figure 10. This graph shows the deflection of the bridge model while loading beam B-4 at different levels of transverse post-tensioning force. Note: C = cracked deck slab; R = damaged beam replacement; *P* = load; TPT = transverse post-tensioning. 1 kip = 4.448 kN.

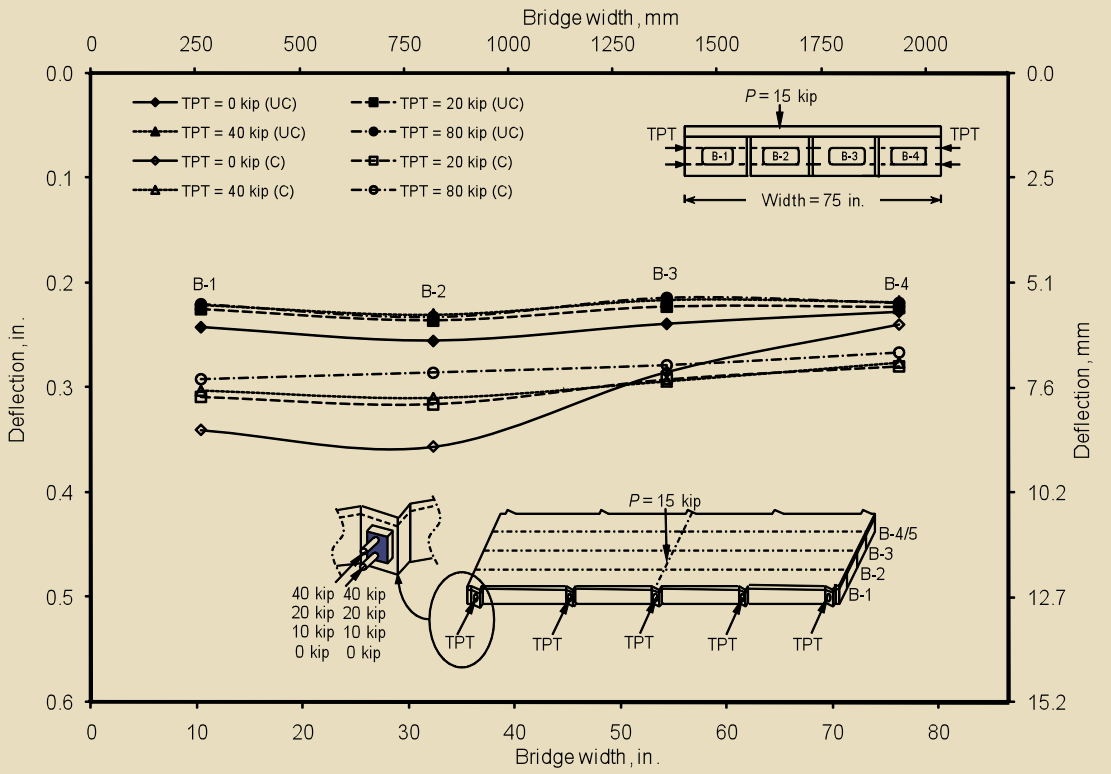

Figure 11. This graph shows the deflection of the bridge model while loading beam B-2 at different levels of transverse post-tensioning force. Note: C = cracked deck slab; *P* = load; TPT = transverse post-tensioning; UC = uncracked deck slab. 1 kip = 4.448 kN.

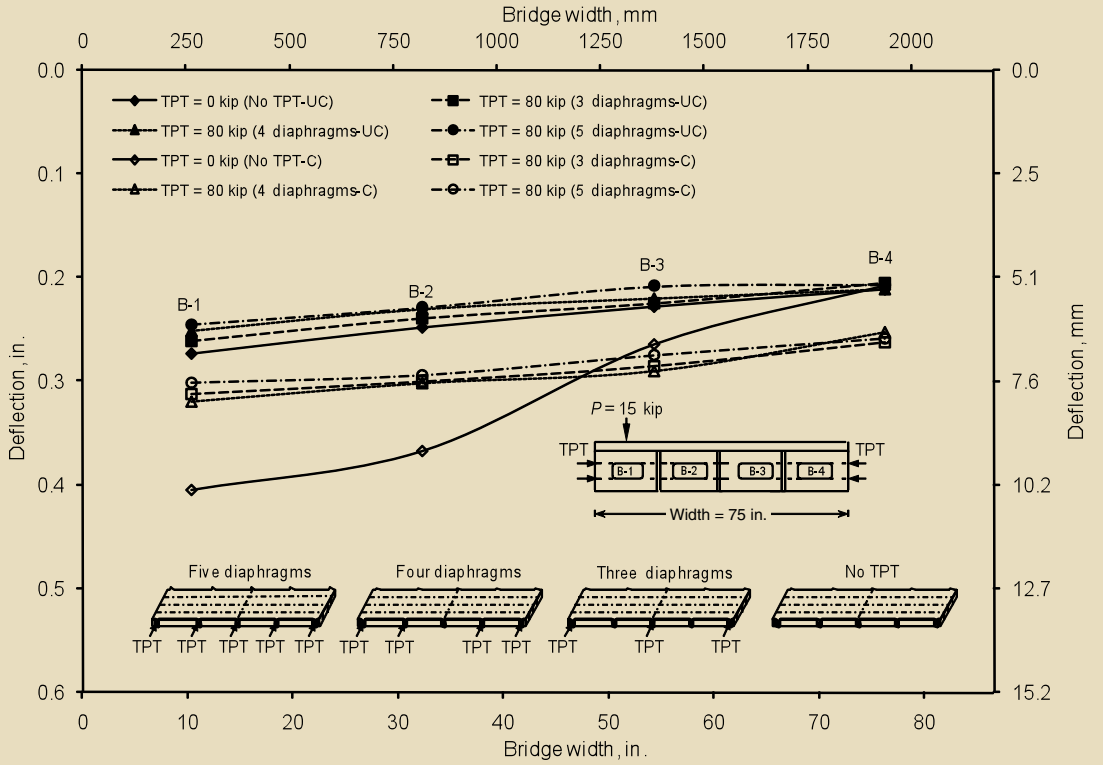

Figure 12. This graph shows the deflection of the bridge model while loading beam B-1 with a different number of diaphragms. Note: C = cracked deck slab; *P* = load; TPT = transverse post-tensioning; UC = uncracked deck slab. 1 kip = 4.448 kN.

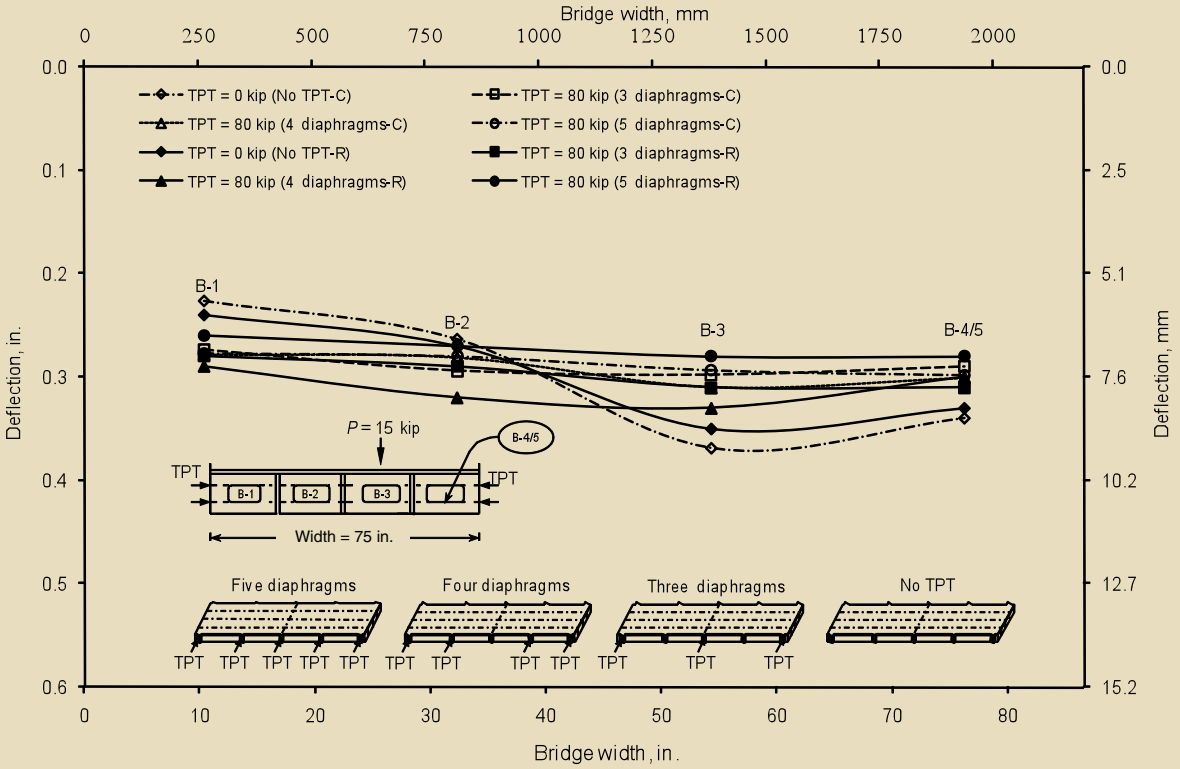

Figure 13. This graph shows the deflection of the bridge model while loading beam B-3 with a different number of diaphragms. Note: C = cracked deck slab; *P* = load; R = damaged beam replacement; TPT = transverse post-tensioning. 1 kip = 4.448 kN.

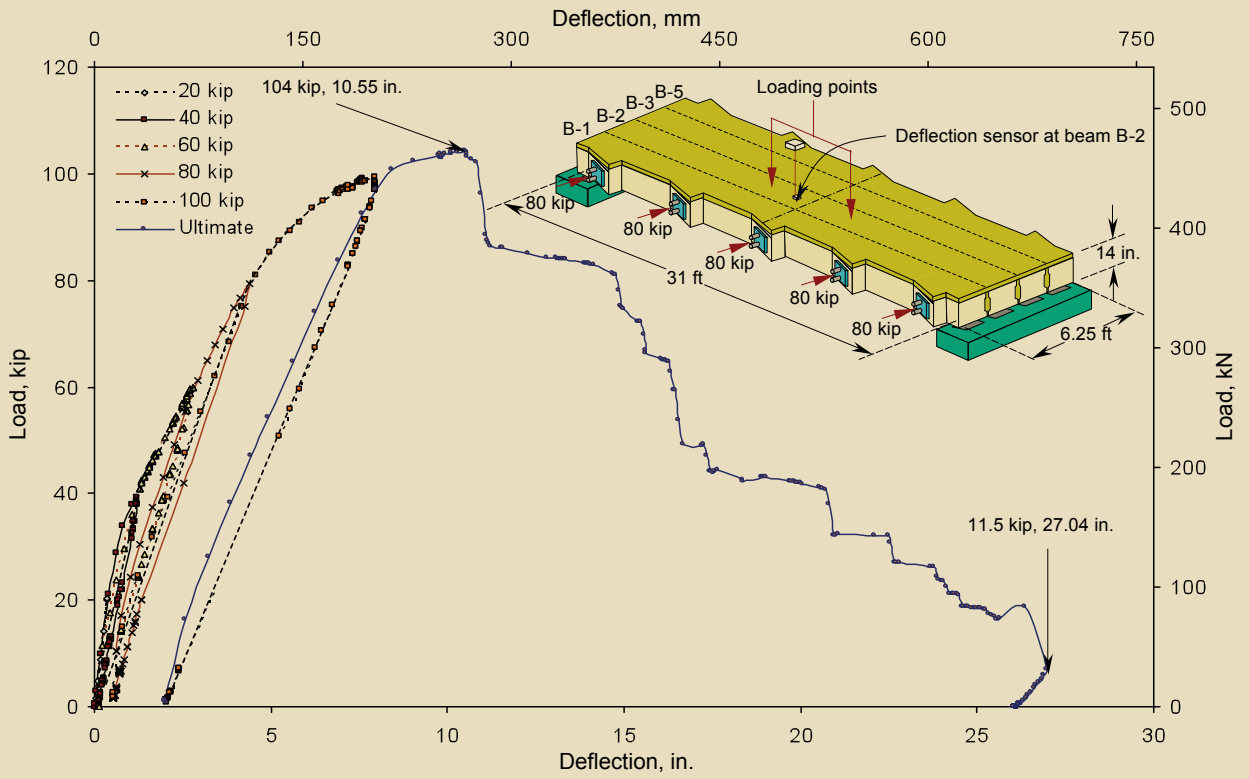

Figure 14. This graph shows the load-deflection response of beam B-2 for different loading and unloading cycles. Note: 1 ft = 0.305 m; 1 kip = 4.448 kN.

cases resulted in lower differences in deflections compared with the four-diaphragm case. Typically, the differences in deflections between box beams B-1 and B-4, when box beam B-1 was loaded in the uncracked phase, were 0.06 in., 0.04 in., and 0.03 in. (1.52 mm, 1.02 mm, and 0.76 mm), corresponding to a transverse post-tensioning force of 80 kip (360 kN) applied to three, four, and five diaphragms, respectively.

However, the differences in deflections between box beams B-1 and B-4 in the cracked phase were 0.05 in., 0.06 in., and 0.04 in. (1.27 mm, 0.52 mm, and 1.02 mm), corresponding to the similar arrangement of transverse post-tensioning. Therefore, the five-diaphragm case outperformed the three-diaphragm case in terms of effectively distributing the applied vertical load, especially in the cracked and the repaired phases of the bridge model.

Ultimate-load test

Load-deflection response The bridge model was loaded eccentrically at the midspan of box beam B-2 with different loading and unloading cycles. **Figure 14** shows the load-deflection response for box beam B-2. The ultimate load-carrying capacity of the bridge model was 104 kip (462 kN), and the corresponding deflection for beam B-2 was 10.55 in. (268 mm). The maximum deflection observed for box beam B-2 was 27.04 in. (687 mm). During the ultimate load cycle, it was observed that all box beams deflected simultaneously regardless of the levels of the applied load until the complete failure of the bridge model occurred.[14]

Failure mode The mode of failure was a typical ductile flexural failure for the entire bridge model. The failure started by initiation and propagation of the flexural tensile cracks at the soffit of the box beams in the midspan region. This was followed by yielding of the bottom reinforcement, which resulted in large deformation of the bridge model near the area of constant load. The yielding of the bottom reinforcement was followed by crushing of the deck-slab concrete across the entire width of the bridge model near the midspan (**Fig. 15**). All four box beams failed simultaneously, which demonstrated the effectiveness of the unbonded transverse post-tensioning arrangement in forcing the bridge model to act as one unit.

When the unbonded CFCC strands used for transverse post-tensioning were removed, it was clear that none of the CFCC strands experienced any permanent deformation or even rupture during the ultimate-load test, even after complete failure of the bridge model. In addition, it was observed that the strands located at the midspan diaphragm experienced the largest increase in transverse post-tensioning force.

Figure 15. This photo shows the failure of the bridge model.

The bottom strand experienced a larger increase in the transverse post-tensioning force than the top strand within the same diaphragm. The largest increase in the transverse post-tensioning force of 2.29 kip (10.2 kN) was observed at the bottom strand located at the midspan diaphragm. This increase was about 9% above the transverse post-tensioning level, which corresponded to an elongation of 8%. However, the strand was still only stressed to 54% of its ultimate guaranteed capacity.

Conclusion

From the tests conducted on the half-scale, 30-deg-skewed, precast, prestressed concrete side-by-side box-beam bridge model, the following results and conclusions are presented:

- Increasing the levels of transverse post-tensioning forces proportionally increases the transverse strains for all points located along the post-tensioned diaphragms. The linear relation between the level of the transverse post-tensioning forces and the corresponding transverse strains reflects the elastic behavior of the concrete.

- Increasing the number of transverse diaphragms, spaced at 7.5 ft and 15 ft (2.29 m and 4.57 m), has an insignificant influence on transverse strain developed on the region between the diaphragms. The low transverse strains indicate a nonuniform distribution of the transverse post-tensioning forces along the entire span of the bridge. None of the arrangements of transverse post-tensioning satisfied the minimum transverse prestress of the AASHTO LRFD specifications limit along the entire length of the bridge.

- The level of transverse post-tensioning forces and the number of transverse diaphragms did not significantly affect the load-distribution behavior of the bridge model in the uncracked-deck-slab phase. However, significant improvement of the load-distribution behavior was observed in the cracked-deck-slab phase.

- The proposed approach for the replacement of a damaged beam using unbonded transverse post-tensioning CFCC strands was successfully implemented. The replacement of the damaged beam and reconstruction of the deck slab and shear key restored the behavior of the bridge model by reducing the deflection of box beams B-3 and B-5. The effect was pronounced at larger numbers of transverse diaphragms and higher levels of transverse post-tensioning forces.

- The failure mode was ductile flexural failure for the entire bridge model (all four box beams). No differential deflection was observed between the adjacent box beams, and no rupture of any unbonded CFCC strands used for transverse post-tensioning was observed after the complete failure. The unbonded transverse post-tensioning arrangement, coupled with the concrete deck slab, distributed the applied eccentric load in the transverse direction until the complete failure of the bridge model.

- The use of unbonded CFCC strands is suitable for transverse post-tensioning applications in side-by-side box-beam bridge systems. The combination of unbonded CFCC strands and transverse diaphragms facilitates the replacement of damaged box beams and allows restoration of strength in box-beam bridges.

- The use of oval-shaped ducts to accommodate unbonded CFCC strands used for transverse post-tensioning can overcome the misalignment problem resulting from differential camber between adjacent box beams.

Acknowledgment

The experimental program presented in this paper was conducted at the Center for Innovative Materials Research (CIMR) at Lawrence Technological University in Southfield, Mich., through the generous support of the Michigan Department of Transportation (MDOT) and the Federal Highway Administration (FHWA) (contract number 2004-0105). The support and comments provided by the MDOT research committee are gratefully appreciated.

References

1. New York State Department of Transportation (NYSDOT). 1992. *Modifications of the Current Shear Key and Tendon System for Adjacent Beam Prestressed Concrete Structures*. Engineering Instruction 92-010: pp. 1–6. Albany, NY: NYSDOT.

2. Gilbertson, G., U. Attanayake, T. M. Ahlborn, and H. Aktan. 2006. *Prestressed Concrete Box-Beam Bridge Performance: Condition Assessment and Design*

Analysis. 06-2432: pp. 22–23. Washington, DC: Transportation Research Board.

3. Huckelbridge, A. A., H. El-Esnawi, and F. Moses. 1995. Shear Key Performance in Multibeam Box Girder Bridges. *Journal of Performance of Constructed Facilities*, V. 9, No. 4 (November): pp. 271–285.

4. Fam, A. Z., S. H. Rizkalla, and G. Tadros. 1997. Behavior of CFRP for Prestressing and Shear Reinforcements of Concrete Highway Bridges. *ACI Structural Journal*, V. 94, No. 1 (January–February): pp. 77–86.

5. American Concrete Institute (ACI) Committee 440. 2003. *Guide for the Design and Construction of Concrete Reinforced with FRP Bars*. ACI 440.1R-03. Farmington Hills, MI: ACI.

6. Grace, N. F., and S. B. Singh. 2003. Design Approach for Carbon Fiber-Reinforced Polymer Prestressed Concrete Bridge Beams. *ACI Structural Journal*, V. 100, No. 3, (May–June): pp. 365–376.

7. Grace, N. F., F. C. Navarre, R. B. Nacey, and W. Bonus. 2002. Design-Construction of Bridge Street Bridge—First CFRP Bridge in the United States. *PCI Journal*, V. 47, No. 5 (September–October): pp. 20–35.

8. Maryland State Highway Administration (MDSHA). 2001. *Maryland Study, Vehicle Collision with Highway Bridges*. Baltimore, MD: MDSHA.

9. Michigan Department of Transportation (MDOT) Design Manual. 2006. Prestressed Concrete Box Beam Details and Post-Tensioning Details. MDOT Bureau of Highway Development, Lansing, MI: MDOT.

10. MDOT. 2007. *Materials Source Guide*. Lansing, MI: MDOT.

11. Hanson, J. Q. 2008. Effect of Level of Transverse Post-Tensioning Forces on the Behavior of Side-by-Side Box-Beam Bridges Using Unbonded CFRP Strands. M.Sc. thesis. Lawrence Technological University, Southfield, MI.

12. Soliman, E. M. 2008. Effect of Number of Diaphragms on the Behavior of Side-by-Side Box-Beam Bridges Using Unbonded Transverse Post-Tensioning CFRP Strands. M.Sc. thesis. Lawrence Technological University, Southfield, MI.

13. American Association of State Highway and Transportation Officials (AASHTO). 2005. *AASHTO LRFD Bridge Design Specifications, 3rd Edition—2005 Interim Revisions*. 3rd ed. Washington, DC: AASHTO.

14. Grace, N., E. Jensen, V. Matsagar, M. Bebawy, E. Soliman, and J. Hanson. 2008. *Use of Unbonded CFCC for Transverse Post-tensioning of Side-by-Side Box-Beam Bridges*. pp. 265–272. Construction and Technology Division of MDOT, Lansing, MI.

About the authors

Nabil F. Grace is a University Distinguished Professor, dean of Engineering, and the director of the Center for Innovative Materials Research at Lawrence Technological University in Southfield, Mich.

Elin A. Jensen is an associate professor and associate dean of engineering for Lawrence Technological University.

Tsuyoshi Enomoto is engineer, manager for the Carbon Fiber Cable Department of the New Business Development Division of the Tokyo Rope Manufacturing Co. Ltd. in Tokyo, Japan.

Vasant A. Matsagar is a post-doctorate research fellow for the Department of Civil Engineering at Lawrence Technological University.

Eslam M. Soliman is a research assistant for the Department of Civil Engineering at Lawrence Technological University.

Joseph Q. Hanson is a research assistant for the Department of Civil Engineering at Lawrence Technological University.

Synopsis

This paper presents the effects of the number of transverse diaphragms and the level of transverse post-tensioning forces using unbonded carbon-fiber-reinforced-polymer (CFRP) strands on the behavior of side-by-side box-beam bridges. An experimental program, consisting of load- and strain-distribution tests, was conducted on a half-scale, 30-deg-skew, side-by-side box-beam bridge model. The bridge model was tested under three different phases: uncracked deck slab, cracked deck slab, and replaced beam.

An ultimate-load test was conducted to evaluate the response of the unbonded transverse post-tensioning arrangement up to failure of the bridge model. The experimental results show that increasing the level of transverse post-tensioning forces generally improved the flexural behavior of the bridge model. Moreover, the different arrangements of the transverse post-tensioning forces had insignificant influence on the transverse strains developed in the region between the diaphragms. From the results of the ultimate-load test, it was evident that the unbonded transverse post-tensioning arrangement coupled with the deck slab uniformly distributed the applied eccentric load in the transverse direction until complete flexural failure of the bridge model occurred.

Keywords

Bridge, box beam, camber, carbon-fiber-reinforced polymer, CFRP, load, strain, unbonded transverse post-tensioning.

Review policy

This paper was reviewed in accordance with the Precast/Prestressed Concrete Institute's peer-review process.

Reader comments

Please address any reader comments to *PCI Journal* editor-in-chief Emily Lorenz at elorenz@pci.org or Precast/Prestressed Concrete Institute, c/o *PCI Journal*, 200 W. Adams Street, Suite 2100, Chicago, IL 60606.